



Parks may not be effective enough to improve the thermal environment in Shanghai (China) as our modified H3SFCA method suggests

Peng Zeng^{a,b}, Dachuan Shi^c, Yaoyi Liu^a, Tian Tian^a, Yue Che^{a,*}, Marco Helbich^b

^a School of Ecological and Environmental Sciences, Shanghai Key Lab for Urban Ecological Processes and Eco-Restoration, Institute of Eco-Chongming (IEC), East China Normal University, Shanghai, 200241, China

^b Department of Human Geography and Spatial Planning, Faculty of Geosciences, Utrecht University, Utrecht, CS 3584, the Netherlands

^c Department of Mechanical Engineering, The University of Hong Kong, Pokfulam Road, Hong Kong Special Administrative Region, China

ARTICLE INFO

Keywords:

Cellular population data
Thermal discomfort
Park cooling effect
Multiple accessibility
Supply-demand mismatch

ABSTRACT

Anthropogenic warming and rapid urbanization have exacerbated the deterioration of urban thermal environments, increasing interest in the ability of parks to regulate local climates. However, their potential to mitigate local thermal discomfort and spatial mismatch in supply and demand is poorly understood. We 1) examined the cooling effects of Shanghai's parks via a thermal comfort index, 2) identified the role of parks in improving local thermal environments by comparing thermal discomfort and park cooling capacity, and 3) explored the spatial mismatch between the demand for thermal discomfort mitigation and the supply of park cooling based on multiple park accessibility. The extent of park cooling is inversely related to the level of urbanization, while cooling intensity is positively associated with urbanization. Only 20.65% of the parks effectively mitigate local thermal discomfort, highlighting the need for improvements. Cooling accessibility increases from the city center to the periphery, with 22.70% of areas lacking access to park cooling services within a 15-min radius. Further improvements can enhance the thermal comfort of accessible parks by 49.55%. Priority adaptation is required in old urban areas and key development zones in peripheral urban areas to meet the needs of their large populations. Our study contributes to the study of urban thermal discomfort mitigation via parks in the context of climate adaptation planning.

1. Introduction

The last eight years have been the warmest on record globally [1]. Urban areas, where over 55% of the global population resides, have been particularly affected, with some megacities, such as Shanghai, Paris, and Houston, experiencing temperature increases exceeding 0.5 °C per decade [2]. This has resulted in significant casualties and economic losses [3]. The United Nations has initiated climate resilience planning for urban thermal environments to address these challenges and enhance people's quality of life [4]. Parks, acting as natural cooling locations within cities, are crucial in mitigating thermal stress [5,6]; thus, their accessibility is gaining attention.

Previous studies have assessed park cooling potentials based on temperature data by calculating multiple indicators (e.g., cooling intensity, extent, and distance) through different methods (e.g., measurements based on maximum or accumulative cooling effects) [7–10]. The most popular approach is to measure a park's maximum impact area

[11,12], often operationalized via buffer zones or catchment area analysis [7,13]. The former entails creating buffers outward from the park's boundary and establishing a nonlinear temperature-distance relationship. The park's maximum cooling impact is determined using the curve's first inflection point [8,13]. In contrast, the catchment area uses gridded temperature data to calculate park-related spatial temperature changes [7,14], which provides a more accurate representation of a park's cooling impact in complex urban settings compared to buffer zones.

Few studies have explored park cooling from a thermal comfort perspective. Due to the high cost of field observations and the limited coverage by meteorological stations, land surface temperature (LST) retrieved from remote sensing imagery is often used as input to model cooling effects [7,9]. However, observed temperature and LST capture only physical aspects of the urban thermal environment and fail to realistically reflect human perception of thermal stress [15]. Human thermal comfort is influenced by various meteorological factors, such as humidity and radiation, and individual factors, such as clothing and

* Corresponding author. School of Ecological and Environmental Sciences, East China Normal University, Shanghai, 200241, China.

E-mail address: yche@des.ecnu.edu.cn (Y. Che).

<https://doi.org/10.1016/j.buildenv.2024.111291>

Received 24 October 2023; Received in revised form 23 January 2024; Accepted 9 February 2024

Available online 15 February 2024

0360-1323/© 2024 Elsevier Ltd. All rights reserved.

Abbreviations	
LST	Land surface temperature
MTHI	Modified temperature-humidity index
TDCI	Thermal discomfort intensity
PCD	Park cooling distance
PCE	Park cooling extent
PCI	Park cooling intensity
NDMI	Normalized difference moisture index
DMDI	Discomfort mitigation demand index
CUA	Central urban area
SUA	Suburban area
OSUA	Outer suburban area
LCZ	Local climate zone
2SFCA	Two-step floating catchment area
H3SFCA	Huff three-step floating catchment area
MH3SFCA	Modified huff three-step floating catchment area

physical condition [16,17]. Numerous indices have been developed to measure human thermal comfort (e.g., discomfort index, wet-bulb globe temperature, physiological subjective temperature, and physiological equivalent temperature) [15,18]. Moreover, thermal comfort has been found to have significant spatial heterogeneity with LST and observed temperature [19]. Therefore, the incorporation of thermal comfort to quantify spatial differences in park cooling effects is crucial and timely.

Moreover, the following two points suggest the need to further explore the equality of park cooling services in hot weather to further climate-resilient urban planning. First, it is essential to consider the varying effectiveness of different parks in improving local thermal discomfort (i.e., the relationship between local thermal discomfort and park cooling), rather than using the park cooling extent or intensity alone as the sole measure of cooling supply [20,21]. Park cooling intensity can contribute to thermal mitigation according to its cooling extent. Consistent with urban heat or humidity island effects [22,23], thermal comfort beyond a specific threshold (e.g., urban or suburban average thermal comfort) refers to thermal discomfort. Higher values indicate greater local cooling demands and vice versa. An understanding of the role of parks in mitigating local thermal discomfort is vital. Positive local thermal discomfort indicates a need for improvement, even with substantial park cooling contributions. Conversely, the thermal environment in regions with low park cooling effects may require no modification. Clarifying the role of parks in local thermal comfort helps to optimize park internal planning to maximize cooling benefits within limited open land and capital investment [10,24,25].

Second, in addition to clarifying park cooling contributions, it is essential to explore the relationship between population demand for thermal discomfort mitigation and park cooling supply. Some studies have assessed park cooling supply by quantifying the ratio of the cooling population to the total population and the distance the public walks to park cooling extent [13,19,20,26]. Although these studies analyzed park cooling equality, they focused solely on time or distance impedance, overlooking the relationship between park supply magnitude and served population. The gravity-based two-step floating catchment area (2SFCA) [27] and its variants [28–30] consider cost effects and supply-demand mismatches. Subal et al. [31] proposed a modified Huff three-step floating catchment area (H3SFCA) by incorporating spatial impedance and service attractiveness. Additionally, different parks affect thermal comfort differently, so consideration of park thermal discomfort mitigation capacity (i.e., cooling intensity) and the local thermal environment status (i.e., thermal comfort) in the accessibility calculation can help capture spatial disparities in park cooling supply. The above accessibility calculations help identify spatial inequalities in the park supply of thermal discomfort mitigation, they do not account for the

actual local demand for cooling. Local population density and thermal discomfort status can also affect the equality of park cooling service allocation [20,32]. To identify critical areas needing thermal comfort improvement, we must combine population cooling demand with cooling accessibility to map the spatial mismatch.

To address the identified research gaps, our study surpasses existing literature in at least three significant ways: 1) by examining the thermal mitigation effects of parks from a thermal comfort perspective; 2) by prioritizing parks for internal renovation from the perspective of comparing localized thermal discomfort and its improvement through park cooling; and 3) by identifying critical areas requiring enhanced park planning from the perspective of assessing the supply-demand spatial mismatch for park cooling. To achieve our objectives, we integrate thermal discomfort data, park cooling effects, cellular population data, and an improved H3SFCA method. Subsequently, we evaluate the potential of parks to enhance thermal comfort, identifying their role and the influencing factors in local thermal discomfort mitigation. Moreover, we assess spatial inequality in park cooling supply through multiple accessibility measures. Finally, we pinpoint spatial mismatches between population discomfort mitigation demand and park supply. Our findings aim to provide valuable insights for climate-resilient park planning in rapidly urbanizing areas, contributing to the development of effective strategies for addressing thermal discomfort and enhancing the overall urban living environment.

2. Materials and methods

2.1. Study area

Shanghai (120°52′-122°12′ E, 30°40′-31°53′ N), the economic, financial, and trade center of China, had a resident population of 24.76 million in 2022 and the highest per capita income in the country [33]. It has a temperate-no dry season-hot summer climate zone with long, hot, and humid summers [34]. In 2022, it experienced 50 days with temperatures exceeding 35 °C, a 138% increase compared to the last 170 years of records. On seven days, temperatures reached 40 °C, tying the 2017 record [35].

To combat heat-related challenges, Shanghai is expanding its urban park system. Between 1990 and 2021, the city added 312 parks, with plans to double that number in the next five years [36]. However, these parks vary in size and layout, resulting in unequal abilities to mitigate local thermal discomfort [11,37]. This study examines these differences in thermal comfort mitigation across 484 urban parks in Shanghai (Fig. 1) identified by the Shanghai Landscaping & City Appearance Administrative Bureau and Baidu Maps. Shanghai was stratified into three primary zones: the central urban area (CUA), suburban area (SUA), and outer suburban area (OSUA).

2.2. Dataset used in the research framework

We selected park data, road networks, cellular population, and remote sensing images to assess spatial inequality and supply-demand mismatch for thermal discomfort mitigation in Shanghai’s parks. The study was organized into three parts (Fig. 2). First, we measured the park cooling effect by inputting the park data and the modified temperature-humidity index (MTHI) into the D8 algorithm [7]. Typically, the algorithm employs digital elevation model maps for watersheds, assuming water always flows in the direction of the steepest slope within a 9-image element window [14]. Lin et al. [7] drew an analogy between the temperature change structure near the park and the digital elevation change in the area near the river. Consequently, the spatial structure of local MTHI variability caused by the park can be likened to the basin structure depicted on digital elevation model maps. Drawing on this analogy, the calculation of the PCE resembles that of a basin calculation. We substituted the digital elevation model with MTHI as the input. This method is also widely used to determine river cooling effects

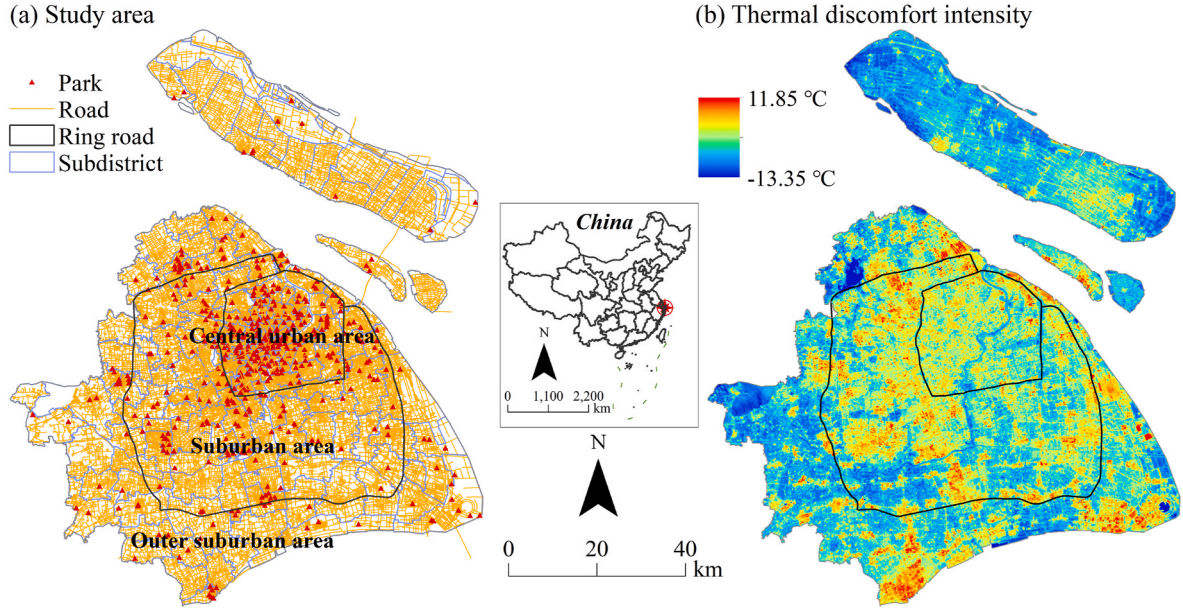


Fig. 1. Study area and the spatial distribution of parks, ring road, road network, subdistricts, and thermal discomfort intensity. Central urban area (CUA), area inside the outer ring road; Suburban area (SUA), area between the outer and suburban ring roads; Outer suburban area (OSUA), area outside the suburban ring road.

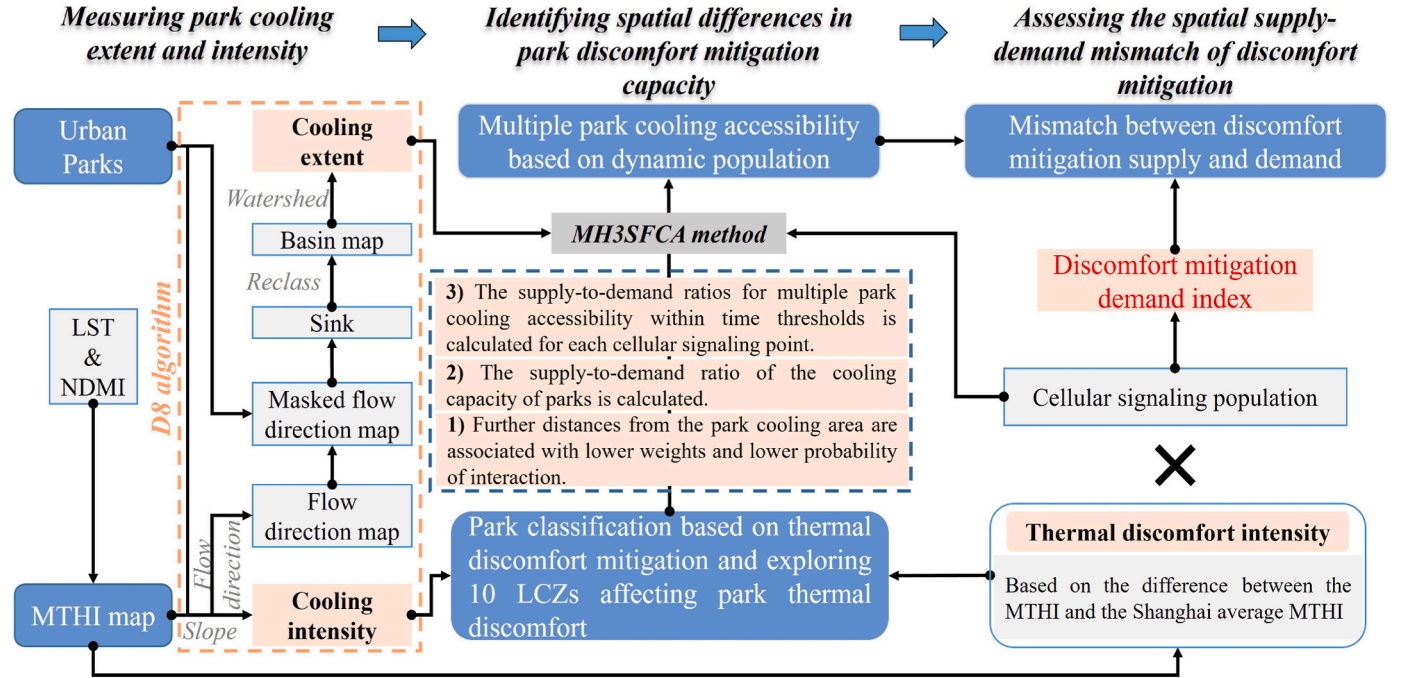


Fig. 2. Research framework.

[14,38,39], suggesting its effectiveness as a tool for exploring cooling effects. The MTHI data were calculated by LST and normalized difference moisture index (NDMI) retrieved from the Landsat 8 remote sensing image on August 14, 2022 (obtained from Geospatial Data Cloud, <https://www.gscloud.cn/>).

Second, we identified the park's role in mitigating local thermal discomfort and its spatial variation. Parks were categorized based on their thermal discomfort mitigation potential, accounting for their cooling capacity and the extent of existing thermal discomfort within their vicinity. We further analyzed the impact of urban landscape attributes, classified as local climate zones (LCZs) [40], on thermal discomfort in different park types. LCZs classify urban forms based on

surface morphology, land function, and human activities, typically delineating ten build-up types and seven land cover types [40]. Exploring the impact of various LCZs on thermal comfort is crucial for enhancing the cooling strategies within parks, particularly from an internal park planning perspective, thereby mitigating public heat stress in Shanghai. According to LCZ maps obtained from the LCZ Generator (<https://lcz-generator.rub.de/>) [41], the build-up LCZs (LCZ₁, LCZ₂, LCZ₃, LCZ₄, LCZ₅, LCZ₆, LCZ₇, LCZ₈, LCZ₉, and LCZ₁₀) and land cover LCZs (LCZ_A, LCZ_B, LCZ_D, and LCZ_G) in Shanghai constituted 62.84% and 37.16%, respectively (Fig. S4). Among them, the top three coverage rankings were LCZD (33.67%), LCZ6 (17.59%), and LCZ8 (14.92%). In terms of the park interior, the build-up LCZs (i.e., LCZ₁, LCZ₂, LCZ₃,

LCZ₄, LCZ₅, LCZ₆, LCZ₈, LCZ₉, and LCZ₁₀) and land cover LCZs (i.e., LCZ_A, LCZ_B, LCZ_D, and LCZ_G) accounted for 59.12% and 40.88%, respectively. The leading three rankings within parks were LCZD (28.70%), LCZ6 (24.12%), and LCZ9 (11.16%) (Table S1). Additionally, we integrated cellular population data from China Unicom, road network data for 2022 from the Shanghai Bureau of Planning and Natural Resources, and park cooling benefits to compute accessibility measures.

Third, we assessed the incongruity between the park thermal discomfort mitigation supply and the corresponding demand. We estimated the population demand for thermal discomfort mitigation in Shanghai by utilizing cellular population data and thermal discomfort intensity. We then identified the spatial mismatch between the demand and park thermal discomfort supply.

We utilized averaged hourly cellular population data for a week (April 12–18, 2023) to reflect the real-time spatial distribution of Shanghai residents. This week featured a mixture of cloudy and sunny conditions, with average temperatures ranging from 16.6 °C to 24.3 °C and excellent air quality. The total cellular population was 26,927,090 individuals, exhibiting a decline from the city center toward the outskirts. The average cellular population densities were 12,908 people/km² (CUA), 5319 people/km² (SUA), and 1578 people/km² (OSUA). Notably, the cellular population in Shanghai is 8.26% higher than the data from the seventh census in 2020 [42]. Given that the smallest census unit is a subdistrict, we conducted calculations for cellular and census populations at the subdistrict level. The two exhibit a substantial positive correlation ($R^2 = 0.78$) (Fig. S2), indicating a similar spatial distribution between cellular and census populations. Additionally, our study's cellular population aligns with the spatial variability observed in widely used publicly available population data sources, such as LandScan in 2022 [43] and WorldPop in 2020 [44] (Fig. S1). These findings collectively suggest that utilizing cellular data as a highly accurate and immediate population input is a reliable approach.

2.3. Calculation of thermal discomfort

Since humidity exacerbates heat stress [15], previous studies have commonly incorporated humidity in the calculation of thermal comfort indices to assess heat stress [45]. The discomfort index (DI), dry-bulb (T_d) and wet-bulb (T_w) temperatures [18], stands out as one of the most widely used indices for thermal comfort assessment. The DI was initially developed based on °F:

$$DI (°F) = 0.4 \times (T_d + T_w) - 15 \quad (1)$$

DI was adapted by Hu et al. [46] as a thermal comfort index (THI) based on observed air temperature (T_{obs} , °C) and relative humidity (RH_{obs} , %):

$$THI (°C) = 1.8 \times T_{obs} + 32 - 0.55 \times (1 - 0.01 \times RH_{obs}) \times (1.8 \times T_{obs} \quad (2)$$

Traditional methods for assessing human thermal comfort rely on meteorological observations. However, these methods fall short in capturing the nuanced thermal variations within urban areas, given the intricate building structures and landscape characteristics [47]. Significantly, Shanghai currently has only ten meteorological stations, and their observations are insufficient for a high-resolution assessment of the spatial variability of thermal comfort in the city. Consequently, our study addresses this limitation by adopting a remote sensing-based MTHI [48]. This index represents an improvement upon conventional urban thermal comfort indices that rely on observed temperature and humidity data [48,49]. The MTHI, modified based on THI, is calculated as follows [48]:

$$MTHI = 1.8 \times T_{rs} + 32 - 0.55 \times (1 - RH_{rs}) \times (1.8 \times T_{rs} - 26) \quad (3)$$

where T_{rs} and RH_{rs} denote LST and NDVI, respectively. LST and NDVI

are highly correlated with near-surface air temperature and meteorological relative humidity, respectively. They are widely employed to improve temperature and relative humidity accuracy in spatial assessments [49–51]. Furthermore, LST and NDVI were computed using Landsat 8 images with a spatial resolution of 30 m, as detailed in Feng et al. [48]. Given that all the parks under investigation in this study exceed 2500 m² in size, the spatial resolution of the Landsat 8 image output proves sufficient for evaluating the thermal comfort effects of parks in Shanghai. To evaluate the appropriateness of MTHI in Shanghai, we calculated the universal thermal climate index at the subdistrict level in Shanghai on August 14, 2022, utilizing *BioKlima 2.6* software (<https://www.igipz.pan.pl/publikacje-zgik.html>) and integrating data from ten meteorological stations. Our analysis revealed a statistically significant positive correlation ($R^2 = 0.74$) between the subdistrict-level MTHI and the universal thermal climate index (see Supplementary Text 1 Verifying the applicability of the modified temperature-humidity index to reflect thermal comfort in Shanghai). Feng et al. [16] also confirmed a significant positive correlation between MTHI and physiological equivalent temperature outcomes. These verification results strongly support the rationale for employing MTHI to explore the fine-grained thermal comfort levels within the study area.

To reflect how parks improve Shanghai's local thermal environment, we took the average MTHI (37.66 °C) as the benchmark for thermal comfort. Thermal discomfort intensity (TDci) was defined as the difference between the MTHI and Shanghai's average MTHI (Fig. 1). A positive or negative TDci indicates that the thermal comfort is above or below the average urban thermal comfort, respectively. Areas with larger negative TDci values indicate a greater need for thermal discomfort mitigation.

2.4. Measurements of park cooling

In this study, MTHI was used to calculate the cooling effect instead of LST, which was commonly used in previous studies [7,14,38]. MTHI was found to manifest higher levels of public heat stress compared to LST across the majority of Shanghai (averaging 3.53 °C ± 1.00 °C higher), with the intensity increasing from highly urbanized to less urbanized areas (Fig. S1). The disparity in heat stress between MTHI and LST within the park exceeded the Shanghai average (0.19 °C higher on average), revealing a subregional ranking of CUA (0.25 °C) > OSUA (0.21 °C) > SUA (0.10 °C). This suggests that the application of MTHI may underestimate the quantification of park cooling effects. Consequently, utilizing MTHI instead of LST proves crucial for a more realistic exploration of park cooling effects from a thermal comfort perspective.

We applied the well-established D8 algorithm [7] to determine the park cooling extent (PCE) and calculate the park cooling intensity (PCI) and distance (PCD). The PCE relies mainly on the MTHI slope and watershed derived from terrain analysis [7,14,38]. We used the 484 parks and the calculated MTHI raster as input. The method for deriving park cooling effects from the MTHI raster using the D8 algorithm is as follows (Fig. 2): Step 1, we utilized the “Flowdirect” command in the ArcGIS hydrological tool to calculate the MTHI “flow direction”; Step 2, we reclassified the MTHI flow direction values to generate the MTHI “sink” and calculated the park area affected based on watershed analysis, employing the “Watershed” command in the hydrological tool; Step 3, to exclude flat areas on the watershed periphery (slope = 0), we applied the “Slope” function in ArcGIS to determine the slope of the MTHI map and overlaid this information on the watershed results to delineate the contour of the “basin”, representing the boundary of the park's cooling effect (i.e., PCE); and Step 4, we extracted the average distance from the park boundary to the PCE boundary and the average MTHI slope within the PCE to derive the PCD and PCI.

2.5. Quantification of park thermal discomfort mitigation supply

We advance the modified Huff three-step floating catchment area

(MH3SFCA) method [31] to quantify multiple thermal discomfort mitigation supplies in parks. MH3SFCA considers the population demand, park supply, and probability of population access to parks [31]. Its calculation consists of three steps: First, we determined the likelihood that a population location selects a specific accessible park within a given distance or time threshold based on the Huff model (i.e., $Huff_{ij}$) [52]. Second, we computed the service supply/demand ratio of parks to the population within the defined threshold range (i.e., R_j). Third, we summarized the service supply/demand ratios of all accessible parks within the threshold range, combining them with their probability of access and the Gaussian modified distance impedance coefficients (used instead of the distance decay function) to determine park service accessibility (i.e., A_j) [32].

We introduce two improvements over Liang et al. [32] and Subal et al. [31]. First, we used an hour-by-hour cellular signaling population lasting one week instead of census population inputs. Previous studies have relied on census residential population data to measure demand [29,31,32]. While these data typically represent the nighttime population, they overlook the daytime population distribution, which likely varies considerably [30,53]. The use of cellular population data to reflect cooling demand can provide a more accurate representation of the geographic population distribution. Second, we used the park cooling extent as the total park supply, integrating park cooling intensity and thermal comfort status. This contrasts with other studies that primarily use park areas as the total supply [30–32]. Our improved method helps to fine-map spatial differences in park thermal discomfort mitigation supply. A 15-min time threshold is considered acceptable [54–56], so it is used to explore the accessibility of multiple travel modes (i.e., walking, biking, e-biking, and driving) (see Supplementary Text 2 How the mode-specific thresholds are determined). The main equations are as follows:

$$\begin{cases} A_i(PCE) = \sum_{k=1}^N \sum_{ic[d_{ij}(M_k) \leq d_0(N)]} Huff_{ij} \times G(d_{ij}(M_k), d_0(N)) \times R_j \\ A_i(PCI) = \sum_{k=1}^N \sum_{ic[d_{ij}(M_k) \leq d_0(N)]} Huff_{ij} \times G(d_{ij}(M_k), d_0(N)) \times R_j \times PCI_j \\ A_i(TDcI) = \sum_{k=1}^N \sum_{ic[d_{ij}(M_k) \leq d_0(N)]} Huff_{ij} \times G(d_{ij}(M_k), d_0(N)) \times R_j \times TDcI_j \end{cases} \quad (4)$$

where $Huff_{ij}$ represents the probability that the population in cellular population grid i travels to park j to obtain service; R_j is the service capacity of park j ; G is the distance decay coefficient based on a Gaussian function; and PCI_j and $TDcI_j$ are the cooling intensity and thermal discomfort intensity within the cooling extent of park j . The equations for $Huff_{ij}$, R_j , and G are:

$$Huff_{ij} = \frac{PCE_j \times G(d_{ij}(M_k), d_0(N))}{\sum_{ic[d_{ij}(M_k) \leq d_0(N)]} PCE_i \times G(d_{ij}(M_k), d_0(N))}, \quad (5)$$

$$R_j = \frac{PCE_j}{\sum_{k=1}^N \sum_{ic[d_{ij}(M_k) \leq d_0(N)]} Huff_{ij} \times CSPop_{iM_k}}, \quad (6)$$

$$G(d_{ij}(M_k), d_0(N)) = \begin{cases} \frac{e^{-0.5 \times (d_{ij}(M_k)/d_0(N))^2} - e^{-0.5}}{1 - e^{-0.5}}, & d_{ij}(M_k) \leq d_0(N) \\ 0, & d_{ij}(M_k) > d_0(N) \end{cases} \quad (7)$$

where N represents the travel mode; $N = 1, 2, 3$, and 4 represents travel via walking, bike, e-bike, and car, respectively; PCE_j is the cooling extent of park j ; $CSPop_{iM_k}$ is the number of people in cellular population grid i that can reach park j within 15 min; $d_{ij}(M_k)$ is the travel distance from cellular population grid i to park j ; and $d_0(N)$ is the distance threshold for

travel mode N .

2.6. Exploration of the impact factors of park thermal discomfort and the supply-demand mismatch for thermal discomfort mitigation

To explore the urban landscape patterns that influence park thermal discomfort, we calculated the percentage of different LCZs in parks and computed their Pearson correlations with park TDcI. Furthermore, we assessed the spatial mismatch between the park thermal discomfort mitigation supply and the demand for human thermal discomfort mitigation via bivariate Moran's I [29,57]. This method is widely used to assess the spatial correlation or dependence between two different spatial variables and is valuable in various fields for understanding complex spatial interactions [32]. The thermal discomfort mitigation supply was determined based on PCE, PCI, and TDcI. Conversely, the thermal discomfort mitigation demand was quantified using the discomfort mitigation demand index (DMDI), which was calculated by multiplying the logged population demand (i.e., cellular population) and the existing thermal discomfort status (i.e., TDcI).

3. Results

3.1. Spatial variation in park cooling

The park cooling results, detailed in Table 1 and illustrated in Fig. 3, unveil significant findings. Notably, a positive correlation exists between PCE and park size. Smaller parks generally exhibit higher PCI and lower PCD than larger parks. Parks in the OSUA rank highest in both PCD and PCI, while CUA parks show the highest average PCE. Specific parks, such as Jiabei Country Park (highest PCE), Xiaotaoyuan Green Park (highest PCI), and Hongqiao Riverside Park (highest PCD) in CUA, stand out for their exceptional cooling attributes. Approximately 77.30% of the study area is accessible via parks, with OSUA having the highest concentration of inaccessible regions at 38.1%. Both PCE-based and PCI-based accessibility exhibit similar spatial patterns, increasing from CUA to OSUA, with only CUA having values lower than the study area's mean. Overall, the inclusion of PCI in accessibility calculations reduces spatial variability across subregions.

3.2. Park types based on thermal discomfort mitigation

In our effort to understand the role of parks in mitigating local thermal discomfort, the 484 parks in Shanghai have been classified into three distinct types based on mean TDcI and PCI within the cooling extent (Fig. 4a and d). Type 1 comprises 382 parks, where thermal discomfort within the cooling extent is yet to be fully mitigated (i.e., $TDcI > 0$). Type 2 includes 37 parks, where thermal discomfort mitigation within the cooling extent is not park-dominated (i.e., $TDcI < 0$ & $TDcI + PCI > 0$). Type 3 encompasses 65 parks, where thermal discomfort mitigation within the cooling extent is park-dominated (i.e., $TDcI < 0$ & $TDcI + PCI < 0$). Type 1 and Type 3 parks are predominantly distributed in CUA, while Type 2 parks are more prevalent in OSUA. Notably, Type 2 parks tend to be larger and have more irregular shapes, signifying that larger and less regularly shaped parks significantly contribute to local thermal discomfort (Table S1). Furthermore, correlation results between park thermal discomfort and landscape patterns suggest that an increase in the proportion of mid- and high vegetation and water body landscapes in Type 1 parks enhances their ability to mitigate local heat discomfort (refer to Supplementary Text 3 Impact of urban landscape patterns on park thermal discomfort). Overall, Type 1 parks in the CUA are the parks with the most pressing need to enhance their cooling supplies by improving their internal blue-green landscape planning (see Fig. 5).

Table 1

Descriptive statistics for park cooling intensity, extent, distance, and accessibility across different subregions.

		Park's TDcI (°C)	PCE (ha)	PCD (m)	PCI (°C)	PCE-based accessibility	PCI-based accessibility
CUA	Average	0.64	6.95	58.74	0.69	2.80	1.83
	Standard deviation	0.78	7.83	30.40	0.14	3.70	2.27
	Coefficient of variation	0.82	0.89	1.93	4.93	1.32	1.24
SUA	Average	1.05	9.40	55.57	0.66	3.26	2.01
	Standard deviation	0.91	11.07	27.47	0.13	7.68	4.59
	Coefficient of variation	1.15	0.85	2.02	5.08	2.36	0.44
OSUA	Average	0.63	12.31	59.41	0.66	9.57	4.08
	Standard deviation	1.50	19.56	29.54	0.11	49.38	22.28
	Coefficient of variation	0.42	0.63	2.01	6.00	5.16	0.18
Total	Average	0.77	8.94	57.86	0.67	6.81	3.17
	Standard deviation	1.04	12.54	29.33	0.13	37.68	17.07
	Coefficient of variation	0.74	0.71	1.97	5.15	5.53	0.18

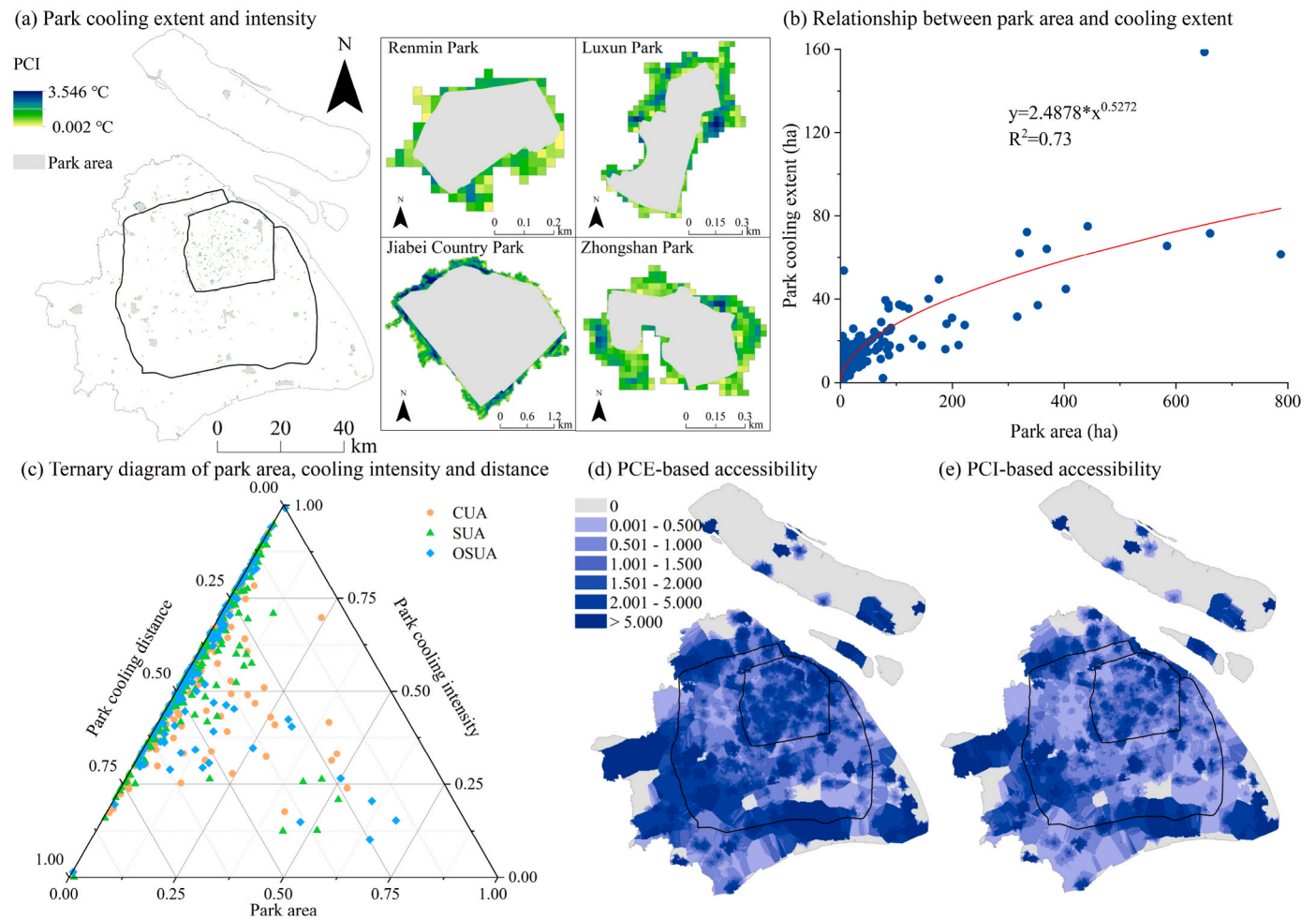


Fig. 3. Spatial variation in park cooling effects and relationships among different indicators. (a) The calculated results of park cooling extents. (b) Relationship between the average park cooling extent and park area. (c) Ternary diagram of the park area, average park cooling intensity, and average park cooling distance. (d) and (e) The calculated results of PCE- and PCI-based accessibility.

3.3. Spatial variation and zoning of accessibility for parks with different thermal discomfort mitigation roles

The spatial variation in different types of park accessibility based on park TDcI was explored in detail (Table 2 & Fig. 4f–h). TDcI-based accessibility for Type 1 parks represents the supply of park thermal discomfort mitigation under above-average urban humid-heat conditions (TDcI > 0), while the opposite holds for Types 2 and 3 (TDcI < 0). The accessibility percentages for Types 1, 2, and 3 parks cover 75.47%,

49.27%, and 54.96% of the study area, respectively, with varying rankings in subregions: SUA > CUA > OSUA for Type 1, OSUA > SUA > CUA for Type 2, and OSUA = SUA > CUA for Type 3. Inaccessible areas for all three types are predominantly located in SUA and OSUA. Notably, Type 2 parks exhibit the greatest spatial heterogeneity in reachability, while Type 1 parks show the least heterogeneity. Combining TDcI-based accessibility for the three park types reveals the spatial pattern of park thermal discomfort mitigation supply in Shanghai (Fig. 4b).

In terms of zoning, based on the park supply for thermal discomfort

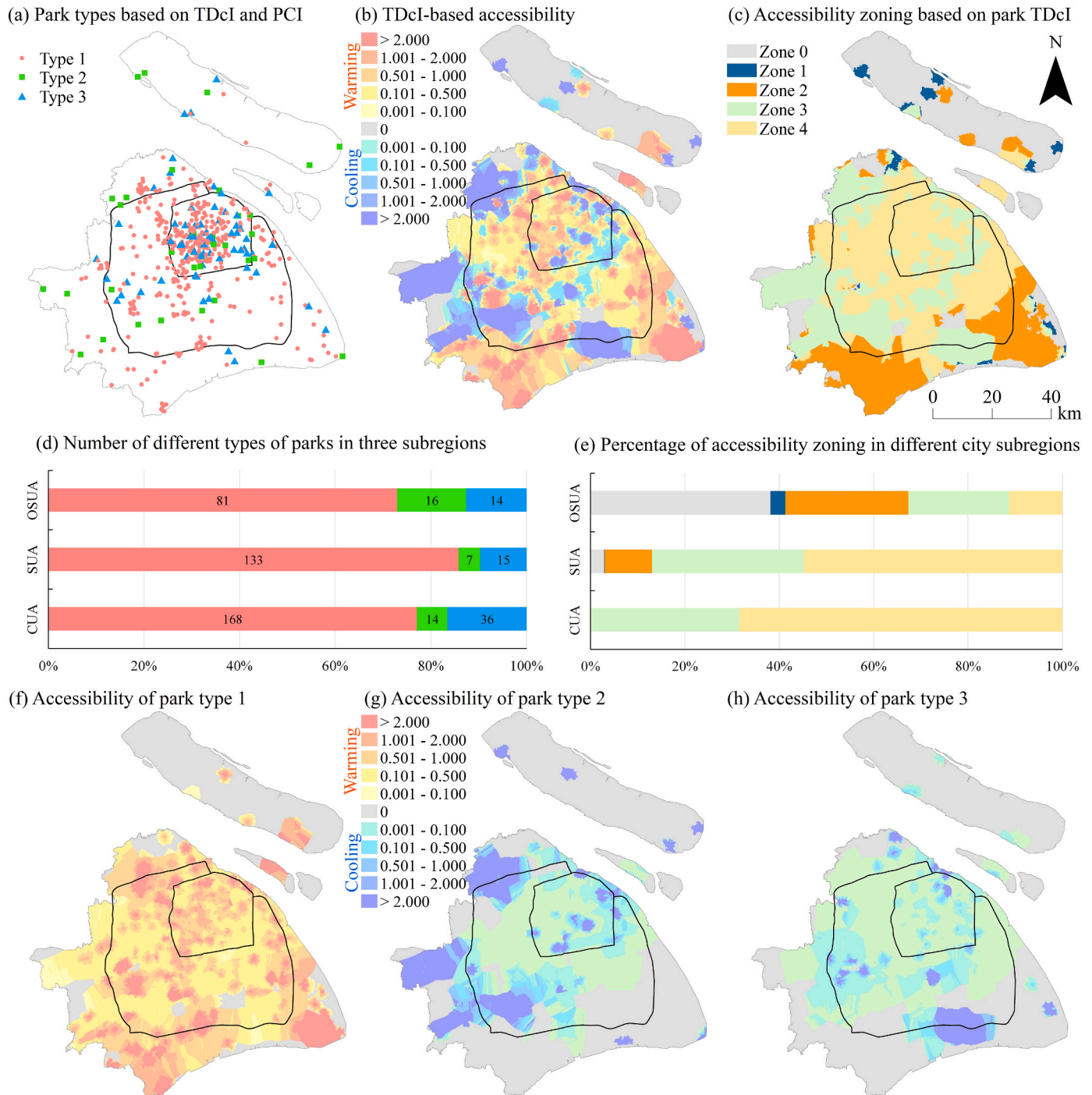


Fig. 4. Spatial distribution and spatial variation in the accessibility of different park types. (a) and (d) Park types based on park cooling intensity versus thermal discomfort within the cooling area in three subregions. (b) The calculated results of TDcI-based park accessibility. (c) and (e) Zoning based on the TDcI-based accessibility of three park types in three subregions. (f)–(h) TDcI-based accessibility of the three park types.

mitigation and no mitigation, the study area was divided into five zones (see Fig. 4c and e): Zone 0 [22.70%], characterized by no accessibility; Zone 1 [1.82%], featuring park supplies for thermal discomfort mitigation only (accessible parks are Type 2 or 3); Zone 2 [18.17%], showcasing park supplies for thermal discomfort nonmitigation only (accessible parks are Type 1); Zone 3 [25.93%], with park accessibility for thermal discomfort mitigation higher than for nonmitigation (the accessibility of park Type 2 or 3 is higher than that of Type 1); Zone 4 [31.38%], presenting a contrast to Zone 3. Zone 1 is predominantly located in southeastern and northern OSUA; Zone 2 is mainly found in

southeastern and southwestern SUA and OSUA. CUA and SUA are dominated by Zone 4, while OSUA is dominated by Zones 0 and 2. Overall, park accessibility for thermal discomfort mitigation varies significantly across urban regions, with Type 1 parks contributing the most in CUA and SUA. Zoning analysis highlights critical areas, indicating diverse spatial patterns and emphasizing the pivotal role of parks in mitigating thermal discomfort in rapidly urbanizing environments. Zones 1 and 2 (i.e., southeast and south Shanghai and Chongming Island) were the most desirable zones for improved park planning.

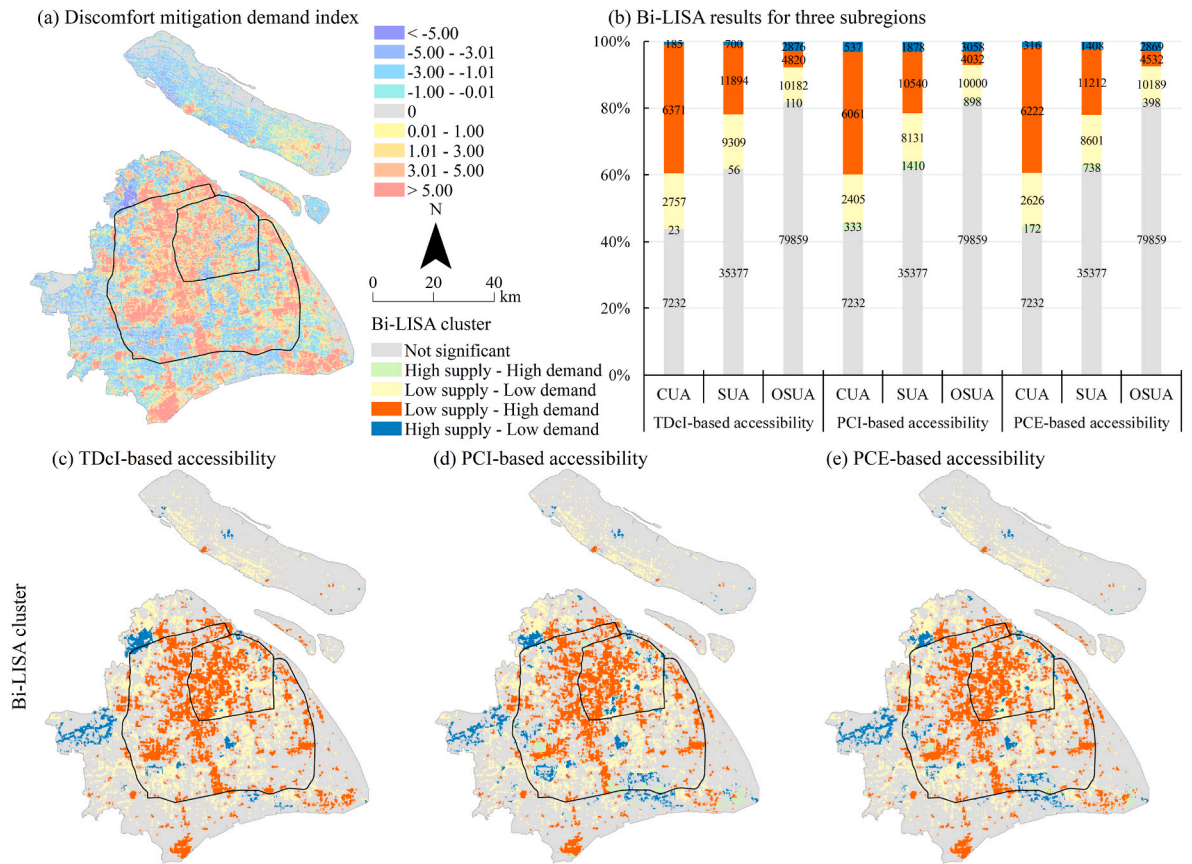


Fig. 5. Supply-demand spatial mismatch of park thermal discomfort mitigation. (a) The calculated results of the discomfort mitigation demand index. (b)–(e) Spatial mismatch between supply and demand based on three park accessibility and discomfort mitigation demand indices.

Table 2
Statistical results for TDcl-based accessibility and the accessibility of three park types in different subregions.

			TDcl-based accessibility	Type 1 accessibility	Type 2 accessibility	Type 3 accessibility
CUA	Percentage (%)	Cooling	31.51	–	99.98	100
		Warming	68.49	100	–	–
		None	0	0	0.02	0
	Value	Average	0.05	0.90	0.74	0.21
		Standard deviation	3.02	1.19	2.56	0.74
		Coefficient of variation	60.40	1.32	3.46	3.52
SUA	Percentage (%)	Cooling	32.32	–	74.59	84.20
		Warming	64.81	96.97	–	–
		None	2.97	3.03	25.41	15.80
	Value	Average	0.41	1.02	0.97	0.40
		Standard deviation	6.37	2.00	5.80	1.56
		Coefficient of variation	15.54	1.96	5.98	3.90
OSUA	Percentage (%)	Cooling	24.51	–	26.65	30.20
		Warming	37.38	58.71	–	–
		None	38.11	41.29	73.35	69.80
	Value	Average	11.65	0.84	8.48	0.40
		Standard deviation	79.60	2.18	75.07	3.56
		Coefficient of variation	6.83	2.60	8.85	8.90
Total	Percentage (%)	Cooling	27.77	–	49.27	54.96
		Warming	49.54	75.47	–	–
		None	22.69	24.53	50.28	45.04
	Value	Average	6.78	0.90	5.22	0.38
		Standard deviation	60.46	2.05	56.89	2.84
		Coefficient of variation	8.92	2.28	10.90	7.47

3.4. Spatial mismatch between park cooling supply and thermal discomfort mitigation demand

A comprehensive analysis of the spatial mismatch between park cooling supply and thermal discomfort mitigation demand was

conducted. Approximately 44.62% of the study area exhibited positive thermal discomfort mitigation needs (DMDI >0), while 35.00% had negative thermal discomfort mitigation needs (DMDI <0), with a decreasing trend from the city center to the peripheral areas. The order of demand in different subregions is CUA (DMDI = 2.42 ± 3.80) > SUA

(DMDI = 3.16 ± 4.11) > OSUA (DMDI = 0.51 ± 3.42). Areas with low supply-high demand anomalies represent the most urgent priority areas for thermal discomfort mitigation. The percentage of low supply-high demand priority areas based on park TDci results is 13.44%, with varying ratios in different urban zones. The spatial characteristics of supply-demand mismatch based on PCE and PCI align with TDci but with slightly lower focus area percentages. This suggests that the supply-demand of thermal discomfort mitigation in CUA and SUA is greatly misaligned and needs urgent improvement. High supply-low demand anomalies are mainly distributed in the western, northern, and southern portions of OSUA, indicating that these local parks have a high capacity to ameliorate thermal discomfort, and their park plans are worth replicating. Overall, these findings underscore the critical importance of addressing thermal discomfort relief in different areas of Shanghai and optimizing park planning to better serve the diverse needs of urban residents.

4. Discussion

4.1. The use of internal planning to increase the role of parks in mitigating local thermal discomfort

This study assessed the role of parks in mitigating thermal discomfort in Shanghai during hot weather. We innovated in using the thermal comfort index to assess parks' role in regulating the urban thermal environment. We found that the thermal comfort index exhibits higher public thermal stress levels than temperature (i.e., LST), and the difference is more pronounced with lower urbanization. In particular, the thermal comfort index overestimates thermal stress inside the park by 5% compared to that outside, with the highest in central Shanghai and the lowest in the suburbs (Fig. S1). This suggests that previous studies relying on LST to evaluate park cooling effects may have overestimated parks' capacity, especially in highly urbanized areas, to ease the urban thermal environment. Therefore, thermal comfort is valuable for a more accurate assessment.

Our study reveals that larger parks in Shanghai generally exhibit a broader cooling range, while smaller parks typically demonstrate higher cooling intensity. Similar findings were observed in Xi'an and Beijing, China [58,59], Wrocław, Poland [60], and Puebla, Mexico [61]. This phenomenon may be attributed to the characteristics of large parks in Shanghai, which are predominantly rural or forested areas in less urbanized regions. These parks boast extensive coverage of blue-green landscapes both inside and outside, and the interaction between these landscapes can enhance the extension distance of the cooling effect, thereby alleviating thermal discomfort [9,62]. Simultaneously, the sparser anthropogenic heat emissions from large parks, compared to smaller ones, contribute to amplifying their cooling range [58]. In contrast, smaller parks are typically situated in highly urbanized central areas with substantial impervious surfaces. The significant temperature differences from their surroundings underscore their capacity to mitigate thermal discomfort in their immediate neighborhoods [59]. It's noteworthy that smaller parks in highly urbanized areas are often developed over an extended period, featuring a vegetative cover predominantly comprising trees and shrubs. This results in superior tree density, lushness, lush area, and tree height compared to large parks in less urbanized areas, consequently facilitating better evapotranspiration and shading [63,64]. Furthermore, enhanced park management practices, such as irrigation, in highly urbanized areas contribute to these parks exhibiting superior vegetation evapotranspiration cooling compared to parks in less urbanized areas [65]. These pieces of evidence clarify why we observe that smaller parks tend to have a higher cooling intensity than their larger counterparts. Numerous studies have enhanced urban thermal environments by augmenting park cooling intensity or coverage [13,26,58]. However, these efforts often overlook the necessity of alleviating local thermal discomfort, making it challenging to assess their effectiveness in mitigating local thermal

discomfort. For example, Xisha National Wetland Park, located on Chongming Island in Shanghai, ranked 470/484 in terms of cooling intensity, but its thermal comfort was better than the Shanghai average by 2.64 °C. In contrast, Zhangyan Park in the southern suburban area ranks 21/484 in cooling intensity but is among the top parks in terms of thermal discomfort (i.e., 4/484, TDci = 3.17 °C). This highlights the inadequacy of prioritizing park planning adjustments solely based on park cooling effects.

We explored the role of parks in mitigating local thermal discomfort based on park cooling supply and thermal discomfort mitigation demand to identify priorities for optimizing park planning. We found that 13% of parks in Shanghai are leaders in mitigating local thermal discomfort, while 8% play supporting roles and share similar priorities. These parks are characterized by a higher percentage of blue space, underscoring the importance of incorporating water features in park designs [12]. In contrast, almost 80% of the parks were ineffective in ameliorating local thermal discomfort. These parks typically feature open buildings and sparse vegetation. Increases in small water features and vegetation near buildings can enhance the cooling capacity in highly urbanized areas. Conversely, improvements can be made in areas with more generous land planning by expanding park size and incorporating larger water features and vegetation. Notably, the Jinshan coastal area in Shanghai's southern periphery, a future urban subcenter with high population density [25], stands out as a critical focus area. The internal landscapes of the six parks in this region exhibit sparse vegetation and medium-to high-rise buildings, ranking in the top ten for thermal discomfort among all 484 parks. Policymakers should prioritize park upgrades in this area to enhance thermal comfort for residents.

4.2. Transitions from identification of to improvements in spatial inequalities between supply and demand in thermal discomfort mitigation

We use a comprehensive approach to assess the equality of public access to park thermal discomfort relief services, considering various factors such as travel modes, park appeal, cooling intensity, and thermal discomfort status. Unlike previous studies that focus exclusively on travel costs and cooling range [13,21,26,66], our analysis revealed several key insights. When looking solely at the cooling extent, we observed that less urbanized areas had lower access to cooling services but higher per capita service intensity, aligning with findings in Wuhan and Shanghai [21,26]. However, when cooling intensity was factored in, per capita cooling service availability decreased, and spatial equality increased. This shift is attributed to the negative correlation between the cooling extent and intensity in Shanghai parks, which reduces spatial variations in the cooling supply. Additionally, by considering the current thermal discomfort of parks, we found that approximately half of Shanghai's population lacks access to park-related cooling services that offer better thermal comfort than the citywide average. This underscores the challenge most parks in Shanghai face in providing excellent thermal comfort.

The combined results of the three accessibility assessments highlight a significant deficiency in cooling service availability for the public in the northern and eastern suburbs, as well as the southern exurbs of Shanghai (Fig. S5). This deficiency is primarily due to the sparse distribution of parks in these regions with limited cooling effects. Notably, most of southeastern Shanghai has parks that are ineffective in improving local thermal comfort, leading to accessibility results that are the opposite of cooling intensity accessibility (Fig. S5). This suggests that despite an increase in the number of parks and per capita service supply in Shanghai over the past two decades [36,67], these efforts have not effectively addressed the worsening thermal environment in Shanghai, which is exacerbated by human-induced warming. Future park planning and redevelopment efforts must prioritize enhancements to the city's climate resilience, particularly in densely populated areas on the city's outskirts.

Furthermore, after considering the population thermal mitigation

demand, the key areas that need to be improved regarding park cooling supply are mainly in the western part of the central city and suburbs. This situation can be explained by the high population density and impervious surface coverage in these regions, which represent Shanghai's traditional urban areas [25], resulting in heightened cooling demand. Additionally, older park designs and traffic congestion in these areas [21] have reduced per capita park cooling accessibility. The "Thousand Parks Project" in Shanghai, which aims to construct or renovate 300 new pocket parks in these areas by 2025 [36], will address this challenge. Moreover, parts of southern central Shanghai (e.g., Minhang Area), western and southern suburbs (e.g., Songjiang and Fengxian Urban Subcenters), and southeastern suburban areas (e.g., Lingang New City) [25] face a severe shortage of thermal discomfort mitigation supply rather than cooling intensity supply. To address this deficiency, several new community parks, country parks, and open recreational woodland parks will be constructed in these areas over the next three years [36]. Our study underscores the importance of renovating existing parks in these regions and emphasizes that planning new parks should prioritize landscaping to enhance local thermal comfort.

In summary, our study demonstrates that the enhanced MH3SFCA-based calculation of multiple accessibility measures provides more comprehensive insights into spatial disparities than prior research. Incorporation of park cooling range thermal comfort into accessibility calculations compensates for the oversight of background thermal conditions in cooling intensity accessibility assessments. By analyzing the mismatch between park cooling supply and the demand for thermal discomfort mitigation, our study offers valuable guidance for decision-makers in formulating targeted spatial planning strategies for urban parks.

4.3. Limitations and future research

Some limitations of this study warrant further refinement. We utilized cellular population data for a week in spring 2023, which may introduce uncertainty due to temporal misalignment with other study data. Future research should consider exploring park cooling supply and demand on different days, given differences in park visitation patterns on weekdays, weekends, and holidays [30,68], as well as population distribution variations during these times [20,69]. Significantly, the population distribution obtained from cellular data over just one consecutive week may be influenced by chance. Therefore, in future studies, we plan to utilize average cellular data over an extended duration, possibly encompassing different seasons. This approach aims to accurately reflect the spatial distribution of the population with high precision, contingent upon considerations of economic cost and data availability. Additionally, the definition of thermal discomfort may affect the results. While the mean thermal comfort value in Shanghai was used in this study, future research could incorporate multiple thresholds to investigate how parks contribute to improving the urban thermal environment across different contexts, such as parks, suburbs, and blue-green spaces [70,71].

5. Conclusions

In the realm of park research, while attention has been directed towards the cooling effects of parks in hot weather, limited exploration exists regarding their capacity to enhance thermal comfort, ensure equitable public access to thermal discomfort relief, and address spatial disparities between the supply and demand for urban thermal mitigation. This study addresses this gap by mapping the distribution of park cooling services during hot weather, quantifying the thermal comfort mitigation effects of 484 parks in Shanghai, assessing their accessibility, and integrating these data with the population's demand for thermal comfort mitigation. Our findings reveal that parks in less urbanized areas of Shanghai exhibit more substantial cooling effects, whereas parks in highly urbanized regions provide greater cooling intensity. This

variation is influenced by both park-specific factors and the surrounding built environment. Specifically, the extended history and effective management of parks in highly urbanized areas have led to substantial internal vegetation cover, predominantly consisting of trees and shrubs, providing excellent shading and evapotranspiration. In contrast, parks in low urbanization areas exhibit a heightened presence of blue-green landscapes both inside and outside, contributing to an expanded scope of cooling impacts. Only 21% of the parks offer a high level of thermal comfort. Dominant parks in local thermal discomfort mitigation are concentrated in the central city and western suburbs, while supporting parks are primarily in the southern parts of the central city and suburban areas. Approximately 72.25% of the population cannot access parks with excellent thermal comfort within a 15-min radius, particularly in the Jinshan Coastal Special Area and Lingang Special Area. Old urban areas, characterized by high demand for thermal discomfort mitigation and low supply, represent crucial areas for enhanced park planning. This study contributes to a more comprehensive understanding of the role of parks in improving the urban thermal environment and carries significant practical implications. It can inform urban climate resilience planning, particularly in the realms of park renovation and equitable space allocation. Furthermore, the data inputs and computational processes employed in this study are generalizable and applicable to regions or countries beyond Shanghai. The research framework is not confined to exploring the supply and demand of park cooling services; it can also be extended to other park service assessments and urban environmental issues such as noise and air pollution.

CRedit authorship contribution statement

Peng Zeng: Writing – original draft, Visualization, Software, Resources, Methodology, Funding acquisition, Formal analysis, Data curation, Conceptualization. **Dachuan Shi:** Writing – review & editing, Methodology, Conceptualization. **Yaoyi Liu:** W. **Tian Tian:** Writing – review & editing, Data curation. **Yue Che:** Supervision, Methodology, Funding acquisition. **Marco Helbich:** Writing – review & editing, Formal analysis, Conceptualization.

Declaration of competing interest

The authors declare that they have no known competing financial interests or personal relationships that could have appeared to influence the work reported in this paper.

Data availability

Data will be made available on request.

Acknowledgments

This research was supported by the program of the Science and Technology Commission of Shanghai Municipality (Grant No. 22dz1208004), the Fundamental Research Funds for the Central Universities (Grant No. 2022ECNU-XWK-XK001 & YBNLTS2023-013). Peng Zeng was funded by the China Scholarship Council (Grant No. 202206140068).

Appendix A. Supplementary data

Supplementary data to this article can be found online at <https://doi.org/10.1016/j.buildenv.2024.111291>.

References

- [1] WMO, State of the Global Climate 2022, World Meteorological Organization, Geneva, Switzerland, 2023, p. 55.

- [2] S.M. Papalexiou, A. AghaKouchak, K.E. Trenberth, E. Foufoula-Georgiou, Global, regional, and megacity trends in the highest temperature of the year: diagnostics and evidence for accelerating trends, *Earth's Future* 6 (1) (2018) 71–79.
- [3] IPCC, Climate change 2022: impacts, adaptation, and vulnerability, in: H.-O. Pörtner, M. Tignor, E.S. Poloczanska, K. Mintenbeck, A. Alegría, M. Craig, S. Langsdorf, S. Löschke, V. Möller, A. Okem, B. Rama (Eds.), *Climate Change 2022: Impacts, Adaptation, and Vulnerability* (D. C. R. Contribution of Working Group II to the Sixth Assessment Report of the Intergovernmental Panel on Climate Change, Cambridge University Press, Cambridge, United Kingdom and New York, NY, USA, 2022, p. 3056.
- [4] United Nations, The Sustainable Development Goals Report 2021, 2021. <https://unstats.un.org/sdgs/report/2021/>.
- [5] J. Hughes, E. Taylor, T. Juniper, Living Cities: towards ecological urbanism, in: Policy Futures Series, Scottish Wildlife Trust, UK, Edinburgh, 2018.
- [6] H. Liu, B. Huang, X. Cheng, M. Yin, C. Shang, Y. Luo, B. He, Sensing-based park cooling performance observation and assessment: a review, *Build. Environ.* 245 (2023) 110915.
- [7] W. Lin, T. Yu, X. Chang, W. Wu, Y. Zhang, Calculating cooling extents of green parks using remote sensing: method and test, *Landsc. Urban Plann.* 134 (2015) 66–75.
- [8] J. Peng, Y. Dan, R. Qiao, Y. Liu, J. Dong, J. Wu, How to quantify the cooling effect of urban parks? Linking maximum and accumulation perspectives, *Rem. Sens. Environ.* 252 (2021) 112135.
- [9] N.H. Wong, C.L. Tan, D.D. Kolokotsa, H. Takebayashi, Greenery as a mitigation and adaptation strategy to urban heat, *Nat. Rev. Earth Environ.* 2 (3) (2021) 166–181.
- [10] Y. Zhou, H. Zhao, S. Mao, G. Zhang, Y. Jin, Y. Luo, W. Huo, Z. Pan, P. An, F. Lun, Studies on urban park cooling effects and their driving factors in China: considering 276 cities under different climate zones, *Build. Environ.* 222 (2022) 109441.
- [11] Y. Li, C. Ren, J.Y. Ho, Y. Shi, Landscape metrics in assessing how the configuration of urban green spaces affects their cooling effect: a systematic review of empirical studies, *Landsc. Urban Plann.* 239 (2023) 104842.
- [12] Z. Yu, G. Yang, S. Zuo, G. Jørgensen, M. Koga, H. Vejre, Critical review on the cooling effect of urban blue-green space: a threshold-size perspective, *Urban For. Urban Green.* 49 (2020) 126630.
- [13] M. Shi, M. Chen, W. Jia, C. Du, Y. Wang, Cooling effect and cooling accessibility of urban parks during hot summers in China's largest sustainability experiment, *Sustain. Cities Soc.* 93 (2023) 104519.
- [14] L. Jiang, S. Liu, C. Liu, Y. Feng, How do urban spatial patterns influence the river cooling effect? A case study of the Huangpu Riverfront in Shanghai, China, *Sustain. Cities Soc.* 69 (2021) 102835.
- [15] J.R. Buzan, K. Oleson, M. Huber, Implementation and comparison of a suite of heat stress metrics within the Community Land Model version 4.5, *Geosci. Model Dev. (GMD)* 8 (2) (2015) 151–170.
- [16] R. Peng, F. Wang, S. Liu, W. Qi, Y. Zhao, Y. Wang, How urban ecological land affects resident heat exposure: evidence from the mega-urban agglomeration in China, *Landsc. Urban Plann.* 231 (2023) 104643.
- [17] P. Zeng, F. Sun, Y. Liu, C. Chen, T. Tian, Q. Dong, Y. Che, Significant social inequalities exist between hot and cold extremes along urban-rural gradients, *Sustain. Cities Soc.* 82 (2022) 103899.
- [18] E.C. Thom, The discomfort index, *Weatherwise* 12 (2) (1959) 57–61.
- [19] J. Dong, J. Peng, X. He, J. Corcoran, S. Qiu, X. Wang, Heatwave-induced human health risk assessment in megacities based on heat stress-social vulnerability-human exposure framework, *Landsc. Urban Plann.* 203 (2020) 103907.
- [20] Y. Xiao, Y. Piao, W. Wei, C. Pan, D. Lee, B. Zhao, A comprehensive framework of cooling effect-accessibility-urban development to assessing and planning park cooling services, *Sustain. Cities Soc.* 98 (2023) 104817.
- [21] P. Zeng, F. Sun, D. Shi, Y. Liu, R. Zhang, T. Tian, Y. Che, Integrating anthropogenic heat emissions and cooling accessibility to explore environmental justice in heat-related health risks in Shanghai, China, *Landsc. Urban Plann.* 226 (2022) 104490.
- [22] Z. Luo, J. Liu, Y. Zhang, J. Zhou, W. Shao, Y. Yu, R. Jia, Seasonal variation of dry and wet islands in Beijing considering urban artificial water dissipation, *npj Climate and Atmos. Sci.* 4 (1) (2021) 58.
- [23] K. Zhang, C. Cao, H. Chu, L. Zhao, J. Zhao, X. Lee, Increased heat risk in wet climate induced by urban humid heat, *Nature* 617 (2023) 738–742.
- [24] Z. Gao, B.F. Zaitchik, Y. Hou, W. Chen, Toward park design optimization to mitigate the urban heat Island: assessment of the cooling effect in five U.S. cities, *Sustain. Cities Soc.* 81 (2022) 103870.
- [25] Shanghai Municipal People's Government, Shanghai Master Plan 2017-2035, 2018. <https://www.shanghai.gov.cn/newshanghai/xxgk/2035004.pdf> (in Chinese).
- [26] M. Chen, W. Jia, L. Yan, C. Du, K. Wang, Quantification and mapping cooling effect and its accessibility of urban parks in an extreme heat event in a megacity, *J. Clean. Prod.* 334 (2022) 130252.
- [27] W. Luo, F. Wang, Measures of spatial accessibility to healthcare in a GIS environment: synthesis and a case study in Chicago region, *Environ. Plan. B Urban Anal. City Sci.* 30 (6) (2003) 865–884.
- [28] D. Dai, Racial/ethnic and socioeconomic disparities in urban green space accessibility: where to intervene? *Landsc. Urban Plann.* 102 (4) (2011) 234–244.
- [29] S. Hu, W. Song, C. Li, J. Lu, A multi-mode Gaussian-based two-step floating catchment area method for measuring accessibility of urban parks, *Cities* 105 (2020) 102815.
- [30] W. Wu, T. Zheng, Establishing a "dynamic two-step floating catchment area method" to assess the accessibility of urban green space in ShenYang based on dynamic population data and multiple modes of transportation, *Urban For. Urban Green.* 82 (2023) 127893.
- [31] J. Subal, P. Paal, J.M. Krisp, Quantifying spatial accessibility of general practitioners by applying a modified huff three-step floating catchment area (MH3SFCA) method, *Int. J. Health Geogr.* 20 (1) (2021) 9.
- [32] H. Liang, Q. Yan, Y. Yan, Q. Zhang, Using an improved 3SFCA method to assess inequities associated with multimodal accessibility to green spaces based on mismatches between supply and demand in the metropolitan of Shanghai, China, *Sustain. Cities Soc.* 91 (2023) 104456.
- [33] Shanghai Municipal Bureau of Statistics, Shanghai Municipality National Economic and Social Development Statistics Bulletin 2022, 2023. <https://tjj.sh.gov.cn/tjgb/20230317/6bb2cf0811ab41eb8ae397c8f8577e00.html> (in Chinese).
- [34] W. Wu, Z. Yu, J. Ma, B. Zhao, Quantifying the influence of 2D and 3D urban morphology on the thermal environment across climatic zones, *Landsc. Urban Plann.* 226 (2022) 104499.
- [35] Shanghai Meteorological Service, High Temperature in Shanghai 2022, 2022. <http://sh.cma.gov.cn/sh/tqyb/gwqk/> (in Chinese).
- [36] Shanghai Municipal Bureau of Statistics, Shanghai Statistical Yearbook 2022, 2022. <https://tjj.sh.gov.cn/tjnj/20230206/804acea250d44d2187f2e37d2e5d36ba.html> (in Chinese).
- [37] Y. Li, C. Ren, J.Y. Ho, Y. Shi, Landscape metrics in assessing how the configuration of urban green spaces affects their cooling effect: a systematic review of empirical studies, *Landsc. Urban Plann.* 239 (2023) 104842.
- [38] L. Chen, Q. Qi, H. Wu, D. Feng, E. Zhu, Will the landscape composition and socio-economic development of coastal cities have an impact on the marine cooling effect? *Sustain. Cities Soc.* 89 (2023) 104328.
- [39] D. Shi, J. Song, Q. Zhong, S.W. Myint, P. Zeng, Y. Che, Cooling wisdom of 'water towns': how urban river networks can shape city climate? *Rem. Sens. Environ.* 300 (2024) 113925.
- [40] I.D. Stewart, T.R. Oke, Local climate zones for urban temperature studies, *Bull. Am. Meteorol. Soc.* 93 (12) (2012) 1879–1900.
- [41] M. Demuzere, J. Kittner, A. Martilli, G. Mills, C. Moede, I.D. Stewart, J. van Vliet, B. Bechtel, A global map of local climate zones to support earth system modelling and urban-scale environmental science, *Earth Syst. Sci. Data* 14 (8) (2022) 3835–3873.
- [42] National Bureau of Statistics of China, Bulletin of the Seven National Census, 2021. <http://www.stats.gov.cn/tjsj/pcsj/rkpc/7rp/indexch.htm/> (in Chinese).
- [43] K. Sims, A. Reith, E. Bright, J. Kaufman, J. Pyle, J. Epting, J. Gonzales, D. Adams, E. Powell, M. Urban, A. Rose, LandScan Global 2022 [Data Set], Oak Ridge National Laboratory, 2023. <https://doi.org/10.48690/1529167>.
- [44] M. Bondarenko, D. Kerr, A. Sorichetta, A.J. Tatem, Estimates of 2020 Total Number of People Per Grid Square, Adjusted to Match the Corresponding UNPD 2020 Estimates and Broken Down by Gender and Age Groupings, Produced Using Built-Settlement Growth Model (BSGM) Outputs, WorldPop, University of Southampton, UK, 2020. <https://doi.org/10.5258/SOTON/WP00698>.
- [45] M. Sadeghi, R. de Dear, G. Morgan, M. Santamouris, B. Jalaludin, Development of a heat stress exposure metric – impact of intensity and duration of exposure to heat on physiological thermal regulation, *Build. Environ.* 200 (2021) 107947.
- [46] Y. Hu, P. Li, J.G. Yang, Y. Zhu, Applied Meteorology, China Meteorological Press, Beijing, 2005.
- [47] E.R. Kuras, M.B. Richardson, M.M. Calkins, K.L. Ebi, J.J. Hess, K.W. Kintzinger, M. A. Jagger, A. Middel, A.A. Scott, J.T. Spector, C.K. Uejio, J.K. Vanos, B.F. Zaitchik, J.M. Gohlke, D.M. Hondula, Opportunities and challenges for personal heat exposure research, *Environ. Health Perspect.* 125 (8) (2017) 085001.
- [48] L. Feng, M. Zhao, Y. Zhou, L. Zhu, H. Tian, The seasonal and annual impacts of landscape patterns on the urban thermal comfort using Landsat, *Ecol. Indic.* 110 (2020) 105798.
- [49] H. Xu, X. Hu, H. Guan, G. He, Development of a fine-scale discomfort index map and its application in measuring living environments using remotely-sensed thermal infrared imagery, *Energy Build.* 150 (2017) 598–607.
- [50] A. Benali, A.C. Carvalho, J.P. Nunes, N. Carvalhais, A. Santos, Estimating air surface temperature in Portugal using MODIS LST data, *Rem. Sens. Environ.* 124 (2012) 108–121.
- [51] S. Li, L. Qian, J. Wang, Improved Temperature-Humidity Index based on Landsat TM/ETM+ and its response to impervious surface, *Geogr. Geo-Inf. Sci.* 29 (2) (2013) 112–115.
- [52] J. Luo, Integrating the huff model and floating catchment area methods to analyze spatial access to healthcare services, *Trans. GIS* 18 (3) (2014) 436–448.
- [53] S. Guo, C. Song, T. Pei, Y. Liu, T. Ma, Y. Du, J. Chen, Z. Fan, X. Tang, Y. Peng, Y. Wang, Accessibility to urban parks for elderly residents: perspectives from mobile phone data, *Landsc. Urban Plann.* 191 (2019) 103642.
- [54] A.R. Khavarian-Garmsir, A. Sharifi, A. Sadeghi, The 15-minute city: urban planning and design efforts toward creating sustainable neighborhoods, *Cities* 132 (2023) 104101.
- [55] Y. Shen, F. Sun, Y. Che, Public green spaces and human wellbeing: mapping the spatial inequity and mismatching status of public green space in the Central City of Shanghai, *Urban For. Urban Green.* 27 (2017) 59–68.
- [56] L. Wu, S.K. Kim, Exploring the equality of accessing urban green spaces: a comparative study of 341 Chinese cities, *Ecol. Indic.* 121 (2021) 107080.
- [57] L. Anselin, Local indicators of spatial association-LISA, *Geogr. Anal.* 27 (2) (1995) 93–115.
- [58] C. Du, W. Jia, M. Chen, L. Yan, K. Wang, How can urban parks be planned to maximize cooling effect in hot extremes? Linking maximum and accumulative perspectives, *J. Environ. Manag.* 317 (2022) 115346.
- [59] K. Qiu, B. Jia, The roles of landscape both inside the park and the surroundings in park cooling effect, *Sustain. Cities Soc.* 52 (2020) 101864.

- [60] J. Blachowski, M. Hajnrych, Assessing the cooling effect of four urban parks of different sizes in a temperate continental climate zone: Wroclaw (Poland), *Forests* 12 (8) (2021) 1136.
- [61] F. Gomez-Martinez, K.M. de Beurs, J. Koch, J. Widener, Multi-temporal land surface temperature and vegetation greenness in urban green spaces of Puebla, Mexico, *Land* 10 (2) (2021) 155.
- [62] I.A. Smith, M.P. Fabian, L.R. Hutyrá, Urban green space and albedo impacts on surface temperature across seven United States cities, *Sci. Total Environ.* 857 (Pt 3) (2023) 159663.
- [63] M. Jaganmohan, S. Knapp, C.M. Buchmann, N. Schwarz, The bigger, the better? The influence of urban green space design on cooling effects for residential areas, *J. Environ. Qual.* 45 (1) (2016) 134–145.
- [64] Z. Zhang, Y. Lv, H. Pan, Cooling and humidifying effect of plant communities in subtropical urban parks, *Urban For. Urban Green.* 12 (3) (2013) 323–329.
- [65] Z. Yu, S. Xu, Y. Zhang, G. Jørgensen, H. Vejre, Strong contributions of local background climate to the cooling effect of urban green vegetation, *Sci. Rep.* 8 (1) (2018) 6798.
- [66] T. Lan, Y. Liu, G. Huang, J. Corcoran, J. Peng, Urban green space and cooling services: opposing changes of integrated accessibility and social equity along with urbanization, *Sustain. Cities Soc.* 84 (2022) 104005.
- [67] P. Fan, L. Xu, W. Yue, J. Chen, Accessibility of public urban green space in an urban periphery: the case of Shanghai, *Landsc. Urban Plann.* 165 (2017) 177–192.
- [68] Y. Xiao, D. Wang, J. Fang, Exploring the disparities in park access through mobile phone data: evidence from Shanghai, China, *Landsc. Urban Plann.* 181 (2019) 80–91.
- [69] H. Liang, Q. Zhang, Temporal and spatial assessment of urban park visits from multiple social media data sets: a case study of Shanghai, China, *J. Clean. Prod.* 297 (2021) 126682.
- [70] Y. Dong, Z. Ren, Y. Fu, N. Hu, Y. Guo, G. Jia, X. He, Decrease in the residents' accessibility of summer cooling services due to green space loss in Chinese cities, *Environ. Int.* 158 (2022) 107002.
- [71] I.D. Stewart, T.R. Oke, E.S. Kravtsov, Evaluation of the 'local climate zone' scheme using temperature observations and model simulations, *Int. J. Climatol.* 34 (4) (2014) 1062–1080.